

High pressure structural study of fluoro perovskite CsCdF₃ upto 60 GPa: A combined experimental and theoretical study

G. Vaitheeswaran^{1*,2}, V. Kanchana¹, Ravhi. S. Kumar³,

A. L. Cornelius³, M. F. Nicol^{3,4}, A. Svane⁵, N. E. Christensen⁵ and O. Eriksson⁶

¹*Applied Materials Physics, Department of Materials Science and Engineering, Royal Institute of Technology, Brinellvägen 23, 100 44 Stockholm, Sweden*

²*Advanced Centre of Research in High Energy Materials (ACRHEM), University of Hyderabad, Hyderabad 500 046, Andhra Pradesh, India*

³*High Pressure Science and Engineering Center and Department of Physics, University of Nevada, Las Vegas, Nevada 89154, USA*

⁴*Department of Chemistry, University of Nevada, Las Vegas, Nevada 89154, USA*

⁵*Department of Physics and Astronomy, Aarhus University, DK-8000 Aarhus C, Denmark*

⁶*Department of Physics and Materials Science, Uppsala University, Box 590, SE-751 21, Uppsala, Sweden*

(Dated: May 30, 2022)

Abstract

The structural behaviour of CsCdF₃ under pressure is investigated by means of theory and experiment. High-pressure powder x-ray diffraction experiments were performed up to a maximum pressure of 60 GPa using synchrotron radiation. The cubic $Pm\bar{3}m$ crystal symmetry persists throughout this pressure range. Theoretical calculations were carried out using the full-potential linear muffin-tin orbital method within the local density approximation and the generalized gradient approximation for exchange and correlation effects. The calculated ground state properties – the equilibrium lattice constant, bulk modulus and elastic constants – are in good agreement with experimental results. Under ambient conditions, CsCdF₃ is an indirect gap insulator with the gap increasing under pressure.

PACS numbers: 62.50.-p, 61.05.cp, 62.20.de, 71.15.Nc

I. INTRODUCTION

Ternary fluorides with the perovskite crystal structure have been extensively studied over several decades, as they have several potential applications because of their optical properties^{1,2}, high-temperature super-ionic behaviour³, and physical properties, such as ferroelectricity⁴, antiferromagnetism⁵, and semiconductivity⁶. The application of CsCdF₃ in the field of luminescence^{7,8,9} has motivated several experimental and theoretical investigations of defect structures involving 3d transition metal ions.^{10,11,12,13,14,15,16,17,18} Elastic properties, including thermal expansion and acoustical measurements of higher order elastic constants, have been reported^{19,20,21,22}. Perovskite fluorides may exhibit structural phase transitions as function of temperature and pressure.^{23,24,25} The present work is a combined theoretical and experimental study of the ground state and high-pressure properties of CsCdF₃. We present the equation of state resulting from high-pressure diamond-anvil cell experiments up to 60 GPa. The ideal cubic structure is preserved over this entire pressure range. We also present the equation of state, the elastic constants and the electronic structure as obtained from theoretical calculations based on density functional theory using two different approximations for the exchange-correlation functional.

The remainder of the paper is organized as follows. Details of the computational method as well as details of the experimental setup are outlined in section II. The measured and calculated equations of state are presented in section III together with calculated ground state properties and elastic properties. The electronic structure and the pressure variation of the band gap are discussed in section IV. Finally, conclusions are given in section V.

II. COMPUTATIONAL AND EXPERIMENTAL DETAILS

A. The electronic structure method

The total energies and basic ground state properties of CsCdF₃ were calculated by the all-electron linear muffin-tin orbital (LMTO) method²⁶ in the full-potential implementation of Ref. 27. In this method, the crystal volume is split into two regions: non-overlapping muffin-tin spheres surrounding each atom and the interstitial region between these spheres. We used a double κ spdf LMTO basis to describe the valence bands, *i. e.* atom-centered Hankel functions with characteristic decay rate denoted by κ are matched to a linear combi-

nation of products of numerical radial function and spherical harmonics within the muffin-tin spheres. The calculations included the 5s, 5p, 6s, and 5d partial waves for cesium, the 5s, 5p, and 4d partial waves for cadmium, and the 2s and 2p partial waves for fluorine. The exchange correlation potential was calculated within the local density approximation (LDA)²⁸ as well as the generalized gradient approximation (GGA) scheme²⁹. The charge density and potential inside the muffin-tin spheres were expanded in terms of spherical harmonics up to $l_{max}=6$, while in the interstitial region, they were expanded in plane waves, with 14146 waves (energy up to 156.30 Ry) included in the calculation. Total energies were calculated as a function of volume for a (16 16 16) k-mesh containing 165 k-points in the irreducible wedge of the Brillouin zone and were fitted to a second order Birch-Murnaghan equation of state³⁰ to obtain the ground state properties.

The elastic constants were obtained from the variation of the total energy under volume-conserving strains, as outlined in Refs. 31 and 32.

B. Experimental details

Polycrystalline samples of CsCdF₃ were synthesized by the solid state reaction method as described elsewhere.^{3,33,34} For high pressure powder diffraction experiments, samples with a few ruby chips were loaded in a Mao-Bell type diamond anvil cell in a rhenium gasket (135 μm hole diameter and pre-indentation thickness 65 μm). Pressure was generated with 325 μm culet diamonds. Silicone fluid was the pressure transmitting medium.³⁵ X-ray diffraction experiments were performed at Sector 16 ID-B, HPCAT, at the Advanced Photon Source. The pressure inside the diamond anvil cell was determined by the standard ruby luminescence method.³⁶ The incident monochromatic x-ray wavelength was $\lambda = 0.36798 \text{ \AA}$. The x-ray diffraction patterns were recorded on an imaging plate with a typical exposure time of 10-20 s, with an incident beam size of 20 x 20 μm . The distance between the sample and the detector was calibrated using a CeO₂ standard. The patterns were integrated using the Fit2D software program³⁷ and the cell parameters were obtained using the JADE package.

The evolution of diffraction patterns as a function of pressure is shown in Fig. 1. At ambient conditions the cell parameter $a = 4.4669(7) \text{ \AA}$ obtained experimentally agrees well with earlier reports provided in the Inorganic Crystal Structure Data base (ICSD).³⁸ Thermal expansion and temperature dependent structural experiments on CsCdF₃ were performed

earlier by Reddy et al.²⁰ They found that the coefficient of thermal expansion increases with temperature. Rousseau et al.¹⁹ investigated the crystal structure and elastic constants of RbCdF₃, TlCdF₃ and CsCdF₃ using x-ray diffraction and Raman techniques at varying temperatures. They found tetragonal distortions in RbCdF₃ and TlCdF₃ at 124 K and 191 K respectively. No structural phase transition were reported in CsCdF₃ in their temperature dependent study. Investigations by Haussuhl³⁹ showed that temperature induced transitions can be observed in the pseudocubic perovskite CsCd(NO₂)₃, which undergoes a phase transition from *R3* to *Pm3m* symmetry around 464 K.³⁹ These reports indicate that the cubic structure of CsCdF₃ is relatively stable in comparison with RbCdF₃, TlCdF₃ and KMgF₃ for a wide range of temperature from 4 K to 300 K.

Fischer²² investigated the pressure dependence of the second order elastic constants of CsCdF₃ and related fluoroperovskites. He reported a decrease in the force constant in RbCdF₃, which is connected with the instability of the F ions. Such instability has not been noticed for CsCdF₃, however a possible phase transition at high pressure was suggested.²² So far, no high pressure experiments have been reported to elucidate the structural behaviour of CsCdF₃. In a previous work we showed that cubic KMgF₃ is stable up to 40 GPa⁴⁰. If any structural phase transition is to be induced in CsCdF₃, one would expect that pressures above 40 GPa are required. However, the diffraction patterns collected in our experiments show no pressure induced structural transformations up to 60 GPa. That is, similarly to KMgF₃, the cubic phase of CsCdF₃ remains stable up to the highest pressures achieved in our experiments.

The bulk modulus was obtained by fitting the pressure-volume data to a second order Birch-Murnaghan equation of state.³⁰

$$P = \frac{3}{2}B_0 [(V/V_0)^{-7/3} - (V/V_0)^{-5/3}] \cdot \{1 + 3/4(B'_0 - 4)[(V/V_0)^{-2/3} - 1]\}, \quad (1)$$

where B_0 is the bulk modulus and B'_0 its pressure derivative. Least square fitting resulted in a B_0 of 79(3) GPa, with a B'_0 of 3.8. Thus, CsCdF₃ has a slightly higher bulk modulus than KMgF₃ ($B_0 = 71.2$ GPa, $B'_0 = 4.7$)⁴⁰

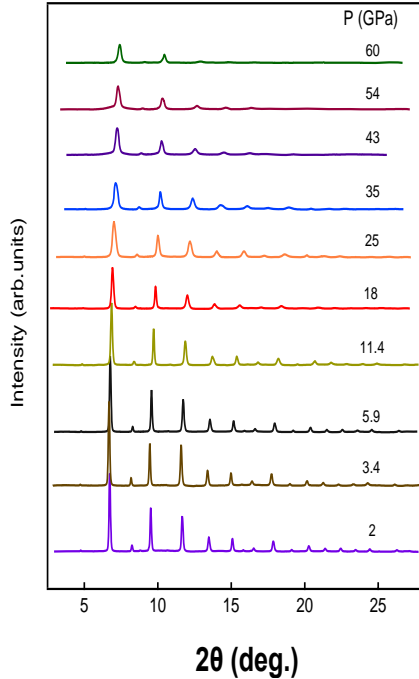


FIG. 1: (Color online) Powder x-ray diffraction patterns of CsCdF_3 recorded at ten pressures up to 60 GPa

III. GROUND STATE AND ELASTIC PROPERTIES

Powder x-ray diffraction patterns collected at several pressures are shown in Figure 1. On compression, the diffraction patterns remain unchanged up to 60 GPa, except for the shifts of diffraction lines caused by the decreasing lattice constant and the broadening due to the intensity decrease with increasing pressure. This implies that no structural transformations occur up to 60 GPa in CsCdF_3 . Figure 2 shows the measured equation of state of CsCdF_3 and compares it with theoretical curves calculated within the LDA and GGA. As is typical, the LDA leads to slightly smaller volume at a given pressure than the experiment, while the GGA gives a larger volume.

The lattice constant and bulk modulus measured in the present work as well as values calculated within the LDA and GGA are given in Table I. Results from earlier experimental works are also quoted for comparison. The bulk modulus obtained in our experiments $B_0 = 79(3)$ GPa with $B'_0 = 3.8$, compares well with values calculated using the LDA. The lattice

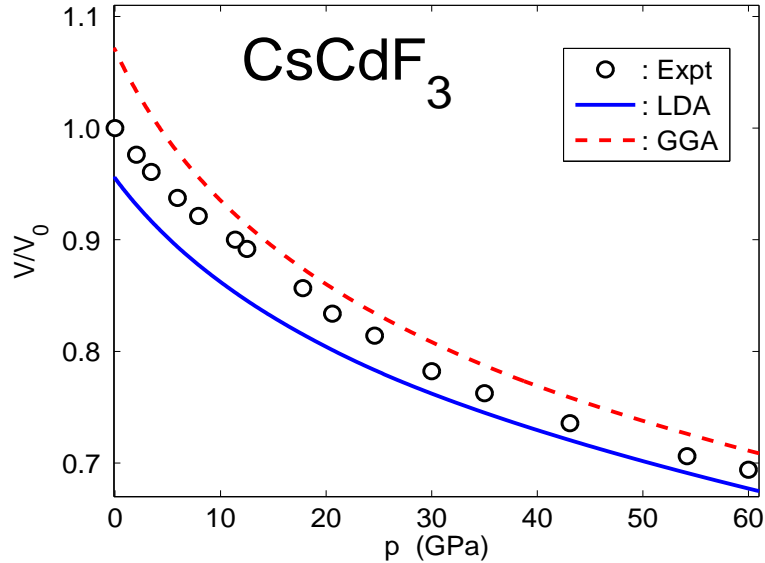


FIG. 2: (Color online) Measured (circles) and calculated (full line: LDA, broken line: GGA) pV -relation of CsCdF_3 .

constant obtained within the LDA is 1.6 % lower than the experimental value, while the corresponding bulk modulus is 4.7% lower than the experimental value, which is the usual level of accuracy of LDA. When comparing the results obtained within GGA, the lattice constant is 2.2 % higher than the experimental value and the corresponding bulk modulus is 32% lower than the experimental value. Since the present theory does not describe thermal effects, it is more relevant to compare to the low temperature experimental lattice constant, which is 0.4 % lower than the room temperature (RT) value (Table I). Further, correcting the low temperature experimental lattice constant for the zero-point motion of the ions, which is not considered in the theory, reduces the best value to compare to theory even more. Hence, the LDA lattice constant is in fact closer to experiment than the GGA value. The excellent agreement between the LDA calculated bulk modulus and the experimental value is, however, fortuitous, since the bulk modulus depends strongly on volume. Due to the overestimated equilibrium volume within GGA (and underestimated with LDA), an error is introduced in the calculated bulk modulus. Therefore, we recalculated the bulk modulus also at the experimental volume, using the simple scaling relation:³¹

$$B(V) = B(V_0) \left(\frac{V_0}{V} \right)^{B'}$$

The corrected values are also quoted in Table I. We find that this diminishes the discrepancies between the LDA and GGA results, as expected. In addition, the LDA bulk modulus now becomes *smaller* than the GGA one for CsCdF₃, and both functionals are seen to actually underestimate the bulk modulus, by approximately 25 % (LDA) and 7 % (GGA).

The elastic constants of CsCdF₃ calculated within LDA and GGA are listed in Table 2 where they are also compared to experimental results as well as earlier calculations. The LDA overestimates the C_{11} value by 28% and the corresponding GGA value is 1.8% lower than the experimental value. The C_{12} value within LDA is 5.4% lower than the experiment, and the corresponding GGA value is 33.3% higher than the experiment. The C_{44} elastic constants are higher by 9% both within LDA and GGA compared to experiment.¹⁹ The C_{11} elastic constant obtained within GGA is much closer to the experimental value than the LDA value, while for C_{12} the situation is reversed, and for C_{11} the two approaches give approximately the same value, and in reasonable agreement with the experimental value. The elastic constants depend sensitively on the volume as illustrated in Figure 3 for the case of LDA. Hence the above values carry an appreciable uncertainty inherited from the volume inaccuracy of the LDA or GGA approach. The pressure derivatives of the elastic constants are more stable quantities. They are compared to experimental values²² in Table III with a reasonable agreement. The C_{11} has the strongest pressure dependence in accordance with the experiment, while the theoretical C_{44} value is almost constant with pressure, while experiment find it increasing with pressure. A point of caution is the fact that the present theory pertains to $T = 0$ K, while experiments are performed at room temperature. Finite temperature generally tends to reduce the elastic constants because of thermal expansion. Using the calculated elastic constants we calculated the anisotropy factor $A = 2C_{44}/(C_{11} - C_{12})$. We find an $A = 0.49$ for LDA and $A = 0.70$ for GGA. The experimental¹⁹ value calculated from the elastic constants is 0.74 which is slightly higher than the GGA value.

IV. ELECTRONIC STRUCTURE

The calculated electron band structure of CsCdF₃ is shown in Figure 4, while the density of states is displayed in Figure 5. The valence bands consist of the fluorine p bands, which dominate the first 2 eV below the valence band maximum. Below these bands appear the

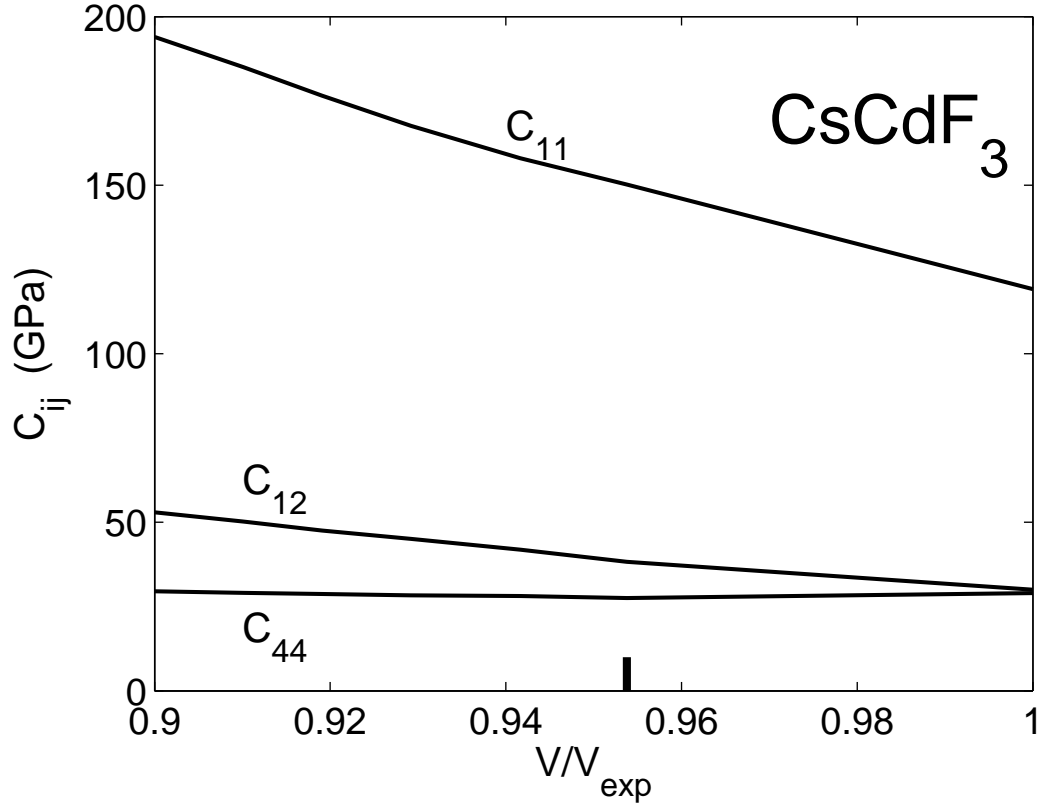


FIG. 3: Volume variation of the elastic constants of CsCdF_3 as calculated in LDA. The volume is given relatively to the experimental volume, while the theoretical LDA equilibrium volume is marked with a vertical bar on the first axis.

Cs 5p bands and the Cd 4d bands, which hybridize heavily in the region from 6 to 4 eV below the top of the valence band. The Cd 6s states dominate the bottom of the conduction band. The insulating gap is calculated to be 3.16 eV in LDA (3.67 eV in GGA). With compression, the gap increases almost linearly, at the rate

$$V \frac{dE_g}{dV} = -2.1 \text{ eV}.$$

The conduction band minimum occurs at the Γ point, while the valence band maximum occurs at the R-point $(1/2, 1/2, 1/2)\frac{2\pi}{a}$, however almost no dispersion is found for the uppermost valence band along the line connecting the R-point with the M-point $(1/2, 1/2, 0)\frac{2\pi}{a}$.

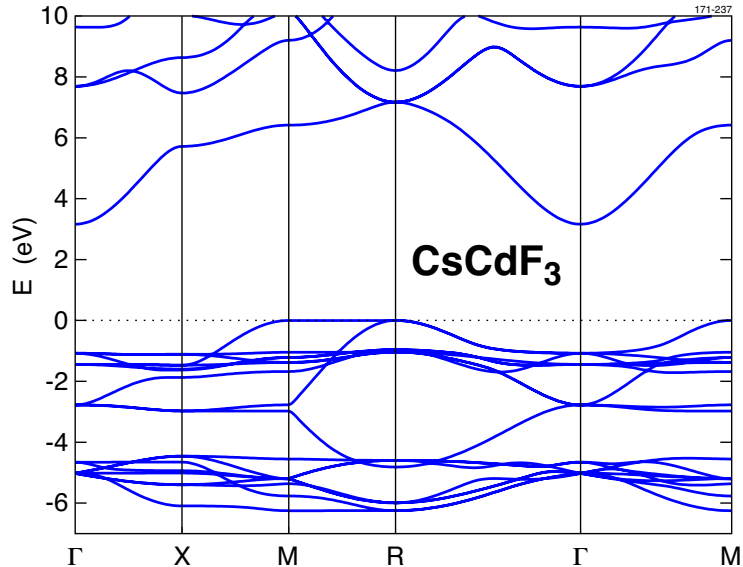


FIG. 4: Band structure of CsCdF₃ (using LDA, at the experimental lattice constant, $a = 4.4669$ Å). The zero of energy is set at the position of the valence band maximum.

V. CONCLUSIONS

In the present work, a combined theoretical and experimental analysis of the structural stability and equation of state of the fluoroperovskite CsCdF₃ has been carried out up to a pressure of 60 GPa. We find that the compound remains in the cubic structure in the entire pressure range studied. The calculated equilibrium lattice constant, bulk modulus and elastic constants agree well with available experimental data. Our electronic structure calculations show that CsCdF₃ is an insulator with an indirect gap which increases with pressure.

Acknowledgments

G. V, V. K acknowledge VR and SSF for financial support and SNIC for providing computer time. Part of the calculations were carried out at the Center for Scientific Computing in Aarhus (CSCAA) supported by the Danish Center for Scientific Computing. The authors gratefully acknowledge the use of the HPCAT facility supported by DOE-BES, DOE-NNSA, NSF, and the W. M. Keck Foundation. HPCAT is a collaboration among the Carnegie In-

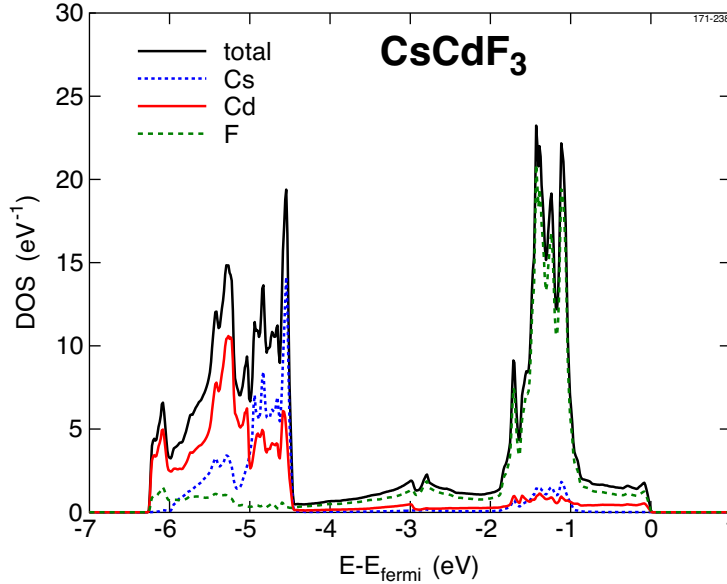


FIG. 5: (Color online) Valence band density of states of CsCdF_3 (using LDA, at the experimental lattice constant). The zero of energy is set at the position of the valence band maximum. The partial projections onto the spheres of Cs, Cd and F are shown with dotted (blue), dashed (red) and dash-dotted (green) lines, respectively, while the full line gives the total density of states. Units are electrons per eV and per formula unit.

stitution, Lawrence Livermore National Laboratory, the University of Nevada Las Vegas, and the Carnegie/DOE Alliance Center. We thank Dr. Maddury Somarazulu and other HPCAT staff for technical assistance. This research was supported from the U.S. Department of Energy Cooperative Agreement No. DE-FC52-06NA26274 with the University of Nevada, Las Vegas.

TABLE I: Lattice constants (in Å), bulk modulus B_0 (in GPa) and its pressure derivative B'_0 , of CsCdF₃ as obtained by experiment and theory. The bulk moduli have been calculated both at the experimental and theoretical volumes ($B_0(V_0^{\text{exp}})$ and $B_0(V_0^{\text{th}})$, respectively)

	Lattice constant	$B_0(V_0^{\text{th}})$	$B_0(V_0^{\text{exp}})$	B'_0
GGA ^a	4.567	53.3	73.6	4.9
LDA ^a	4.397	75.6	59.7	4.9
Expt.(RT)	4.4669(7) ^a , 4.465 ^b , 4.4662 ^c ,		79(3) ^a	3.8 ^a , 5.8 ^d
Expt.($T = 0$ K)	4.452 ^b			

^aPresent work; ^bRef. 19; ^cRef. 20; ^dRef. 22.

TABLE II: Calculated elastic constants and shear modulus (G), all expressed in GPa, of CsCdF₃ at the theoretical equilibrium volume.

	C_{11}	C_{12}	C_{44}	G	
GGA	105.8	27.0	27.7	32.4	Present
LDA	150.2	38.3	27.5	38.9	Present
Expt.	107.8±0.2	40.5±0.5	25.0±0.2	28.5±0.5	Ref. 19

TABLE III: Calculated LDA pressure derivatives of the elastic constants of CsCdF₃ at the experimental equilibrium volume.

	$\frac{dC_{11}}{dp}$	$\frac{dC_{12}}{dp}$	$\frac{dC_{44}}{dp}$	
LDA	8.8	2.9	0.4	Present
Expt.	11.1±0.1	3.2±0.1	2.2±0.4	Ref. 22

-
- * Author for Correspondence, E-mail: vaithee@kth.se
- ¹ G. Hörsch and H. J. Paus, *Opt. Commun.* **60**, 69 (1986).
 - ² R. Hua, B. Lei, D. Xie, and C. Shi, *J. Sol. State Chem.* **175**, 284 (2003).
 - ³ A. V. Chadwick, J. H. Strange, G. A. Ranieri, and M. Terenzi, *Solid State Ion.* **9-10**, 555 (1983).
 - ⁴ P. Berastegui, S. Hull, and S.-G. Eriksson, *J. Phys.: Condens. Matter*, **13**, 5077 (2001).
 - ⁵ J. Julliard and J. Nouet, *Revue de Phys. Appl.* **10**, 325 (1975).
 - ⁶ R. R. Daniels, G. Margaritondo, R. A. Heaton, and C. C. Lin, *Phys. Rev. B* **27**, 3878 (1983).
 - ⁷ B. Villacampa, R. Cases, V. M. Orera and R. Alcalá, *J. Phys. Chem. Sol.*, **55**, 263 (1994).
 - ⁸ B. Villacampa, R. Cases and R. Alcalá, *J. Luminesc.*, **63**, 289 (1995).
 - ⁹ M. T. Barriuso, M. Moreno and J. A. Aramburu, *Phys. Rev. B* **65**, 064441 (2002).
 - ¹⁰ M. E. Ziaei and J. Owen, *J. Phys. C*, **9**, L529 (1976).
 - ¹¹ C. D. Adam, A. H. Harker, and J. Owen, *J. Phys. C*, **12**, L239 (1979).
 - ¹² E. Minner, D. Lovy and H. Bill, *J. Chem. Phys.*, **99**, 6378 (1993).
 - ¹³ M. Springis, A. Sharakovskiy, I. Tale, and U. Rogulis, *phys. stat. sol. (c)* **2**, 511 (2005).
 - ¹⁴ H. Takeuchi, M. Arakawa and H. Ebisu, *J. Phys. Soc. Japan*, **56**, 3677 (1987).
 - ¹⁵ J. S. Yao, S. Y. Wu, X. Y. Gao and H. M. Zhang, *Hyperfine Interact.* **174**, 103 (2007).
 - ¹⁶ J.-H. Li, X.-Y. Kuang, M.-L. Duan and Z.-Y. Jiao, *Solid State Communications* **141**, 279 (2007).
 - ¹⁷ S. Y. Wu, Z. H. Zhang, L. H. Wei, H. Wang, Y. X. Hu, *Chemical Physics* **348**, 199 (2008).
 - ¹⁸ J. A. Aramburu, J. I. Paredes, M. T. Barriuso, and M. Moreno, *Phys. Rev. B* **61**, 6525 (2000).
 - ¹⁹ M. Rousseau, J. Y. Gesland, J. Julliard, J. Nouet, J. Zarembowitch, and A. Zarembowitch, *Phys. Rev. B* **12**, 1579 (1975).
 - ²⁰ K. D. Reddy, P. Kistiah and L. Iyengar, *J. Less-Comm. Met.*, **92**, 81 (1983).
 - ²¹ M. A. Breazeale, J. Philip, A. Zarembowitch, M. Fischer, and Y. Gesland, *Journal of Sound and Vibration* **88**, 133 (1983).
 - ²² M. Fischer, *J. Phys. Chem. Solids*, **43**, 673 (1982).
 - ²³ Y. S. Zhao, *J. Solid State Chem.* **141**, 121 (1998).
 - ²⁴ Y. S. Zhao, J. B. Parise, Y. B. Wang, K. Kusaba, M. T. Vaughan, D. J. Weidner, T. Kikegawa, J. Chen, O. Shimomura, *Am. Mineral.* **79**, 615 (1994).
 - ²⁵ A. R. Chakhmouradian, K. Ross, R. H. Mitchell, and I. Swainson, *Phys. Chem. Minerals* **28**,

- 277 (2001).
- ²⁶ O. K. Andersen, Phys. Rev. B **12**, 3060 (1975).
- ²⁷ S. Y. Savrasov, Phys. Rev. B **54**, 16470 (1996).
- ²⁸ S. H. Vosko, L. Wilk, and M. Nusair, Can. J. Phys. **58**, 1200 (1980).
- ²⁹ J. P. Perdew, K. Burke, and M. Ernzerhof, Phys. Rev. Lett. **77**, 3865 (1996). We use the proposed value $\kappa = 0.804$ in the gradient enhancement factor of this functional.
- ³⁰ F. Birch, Phys. Rev. **71**, 809, (1947).
- ³¹ V. Kanchana, G. Vaitheeswaran, A. Svane and A. Delin, J. Phys.: Condens. Matter, **18**, 9615 (2006);
- ³² V. Kanchana, G. Vaitheeswaran and A. Svane J. Alloys and Compounds **455**, 480 (2008).
- ³³ Y. Zhao, J. Solid State Chem. **141**, 121 (1998).
- ³⁴ R. W. Smith, W. N. Mei, J. W. Flocken, M. J. Dudik, and J. R. Hardy, Mat. Res. Bull. **35**, 341 (2000).
- ³⁵ Y. R. Shen, R. S. Kumar, M. Pravica, and M. F. Nicol, Rev. Sci. Instrum. **75**, 4450 (2004).
- ³⁶ H. K. Mao, J. Xu and P. M. Bell, J. Geophys. Res. **91**, 4673 (1986).
- ³⁷ A. P. Hammersley, S. O. Svensson, M. Hanfland, A. N. Fitch, and D. Häusermann, High Pressure Res. **14**, 235 (1996).
- ³⁸ C. Q. Wu and R. Hoppe, Z. Für An. und Allg. Chem. **514**, 92 (1984).
- ³⁹ S. Haussuhl, Cryst. Res. Tech. **29**, 697 (1994)
- ⁴⁰ G. Vaitheeswaran, V. Kanchana, Ravhi S. Kumar, A. L. Cornelius, M. F. Nicol, A. Svane, A. Delin and B. Johansson, Phys. Rev. B **76**, 014107 (2007).